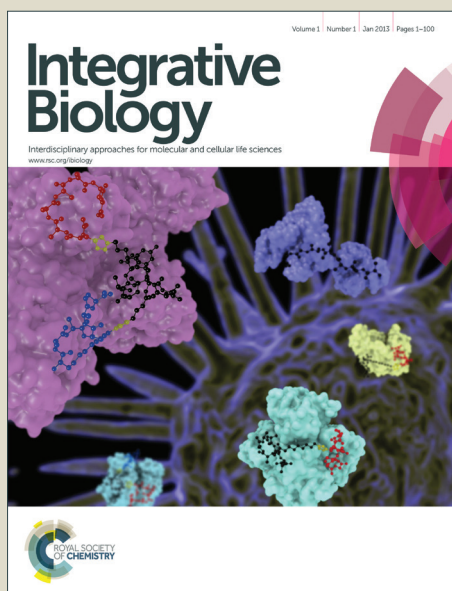


Integrative Biology

Accepted Manuscript



This is an *Accepted Manuscript*, which has been through the Royal Society of Chemistry peer review process and has been accepted for publication.

Accepted Manuscripts are published online shortly after acceptance, before technical editing, formatting and proof reading. Using this free service, authors can make their results available to the community, in citable form, before we publish the edited article. We will replace this *Accepted Manuscript* with the edited and formatted *Advance Article* as soon as it is available.

You can find more information about *Accepted Manuscripts* in the [Information for Authors](#).

Please note that technical editing may introduce minor changes to the text and/or graphics, which may alter content. The journal's standard [Terms & Conditions](#) and the [Ethical guidelines](#) still apply. In no event shall the Royal Society of Chemistry be held responsible for any errors or omissions in this *Accepted Manuscript* or any consequences arising from the use of any information it contains.

Insight Box:

While cell migration plays fundamental roles in many different biological systems, including the immune system, the regulation of this important and complicated cellular function is not fully understood. New innovations in microfluidic technology have enabled us to develop a new screening method to elucidate how the human pathogen *Salmonella* influences the migratory behavior of certain types of immune cells and has already successfully identified 7 *Salmonella* genes that block the migration of these immune cells. By integrating this unique microfluidic technology with cell biology, we now have a fast and reliable screening method to genetically dissect the complex process of cell migration.

Cite this: DOI: 10.1039/c0xx00000x

www.rsc.org/Integrative Biology

PAPER

A microfluidic-based genetic screen to identify microbial virulence factors that inhibit dendritic cell migration

Laura M. McLaughlin,^{§ a,b} Hui Xu,^{§ c} Sarah E. Carden,^b Samantha Fisher,^a Monique Reyes,^a Sarah C. Heilshorn^c and Denise M. Monack^{† b}

Received (in XXX, XXX) Xth XXXXXXXXX 20XX, Accepted Xth XXXXXXXXX 20XX
DOI: 10.1039/b000000x

Microbial pathogens are able to modulate host cells and evade the immune system by multiple mechanisms. For example, *Salmonella* injects effector proteins into host cells and evades the host immune system in part by inhibiting dendritic cell (DC) migration. The identification of microbial factors that modulate normal host functions should lead to the development of new classes of therapeutics that target these pathways. Current screening methods to identify either host or pathogen genes involved in modulating migration towards a chemical signal are limited because they do not employ stable, precisely controlled chemical gradients. Here, we develop a positive selection microfluidic-based genetic screen that allows us to identify *Salmonella* virulence factors that manipulate DC migration within stable, linear chemokine gradients. Our screen identified 7 *Salmonella* effectors (SseF, SifA, SspH2, SlrP, PipB2, SpiC and SseI) that inhibit DC chemotaxis toward CCL19. This method is widely applicable for identifying novel microbial factors that influence normal host cell chemotaxis as well as revealing new mammalian genes involved in directed cell migration.

Introduction

Salmonella enterica serovars are facultative intracellular pathogens that can cause acute gastroenteritis or systemic typhoid fever in humans, a disease that still burdens millions of people per year world-wide¹. *Salmonella* injects effector proteins into host cells through type-III secretion systems (T3SS), which are required for virulence². For example, *Salmonella enterica* serovar Typhimurium (*S. typhimurium*) translocates an effector protein, SseI, that plays a role in modulating DC migration toward the chemokine CCL19^{3, 4}. Normally DCs chemotax toward the T cell zones of secondary lymphoid tissue primarily following the chemokine gradients of CCL19 and CCL21⁵ and help control infection by activating the adaptive immune response⁶. Previously we have identified the *Salmonella* factor SseI as a modulator of DC chemotaxis, however, our findings also suggested that *Salmonella* injects additional factors that influence DC chemotaxis using the *Salmonella* pathogenicity island 2 (SPI2) T3SS³. Approximately 30 *Salmonella* effectors have been documented to be translocated by the SPI2 T3SS² and therefore a screen-based approach would be the most efficient method of determining which of these effectors interfere with DC chemotaxis. The goal of this study was to identify these additional *Salmonella* factors involved in manipulating DC directed migration using novel engineered genetic screening

tools.

Microfluidic techniques provide a vital addition to traditional tissue culture plate-based cell assays by offering more precise temporal and spatial control over the extracellular microenvironment by promoting fast diffusion and efficient mixing on a sub-microliter scale. Because only nano to microliter sample/reagent volumes are necessary, low cost high-throughput testing with expensive or rare clinical samples is achievable. A variety of physical, electrochemical, mechanical or optical detection schemes have been integrated with microfluidic devices for genetic analysis, phenotype screening, cell sorting or cell behavior manipulation at sub-cellular, single-cell and whole organism levels⁷⁻¹⁰. Microfluidic-based sorting and screens of cell populations can be extremely versatile, using detection schemes that are physical (e.g., microfilters, flow based or acoustic focusing), electrochemical (e.g., impedance or potentiometry), mechanical and optical (e.g., fluorophore conjugation of affinity markers, chemiluminescence, bioluminescence, surface plasmon resonance/refractive index)^{7, 9, 11-21}. A variety of microfluidic devices have been developed for gradient generation based on flow and mixing, microjet or restricted passive diffusion through membrane, microcapillaries and hydrogels²²⁻³⁴. Particularly, microfluidic gradient generators have become more readily accepted in addition to traditional chemotactic assays, which have several inherent limitations. The most significant drawback is that the concentration gradient profiles are transient, unstable, and

hard to reproduce in many traditional assays (e.g. micropipette assay,³⁵ Boyden chamber,³⁶⁻³⁸ Zigmond chamber,³⁹ Dunn chamber⁴⁰). Secondly, most conventional chemotaxis assays do not support direct cell migration monitoring and detailed single cell analysis, which are required for quantification of important metrics (such as cell speed and directionality of movement)^{38, 41}. In contrast, modern microfluidic chemotaxis devices provide long-term stable and defined concentration gradients with the possibility of real-time imaging. For shear-sensitive or semi-adherent cell cultures (including DCs), soluble^{25-34, 42} chemical gradients may be generated by passive Fickian chemical diffusion through microcapillaries^{7, 25-27, 42-44}. This device design is also advantageous because specific populations of cells that successfully migrate through the capillaries toward a given chemoattractant may be captured for end-point analysis²⁶. The application of these devices has significantly advanced our understanding of cell migration from neutrophil chemotaxis^{25, 27} to cancer progression²⁶.

Despite the fast development of novel chemotaxis tools, there is still a lack of high-throughput chemotaxis screening methods. Current protocols focus on the analysis of one cell type per assay compartment that may be arranged in a parallel testing format to form miniature assay arrays (such as micro dots⁴⁵ or microchannels⁴⁶). To maximize high-throughput potential, simultaneous monitoring of multiple cell populations with the ability to isolate and capture a targeted population within one single device is needed. Previously, motility based screening has been successfully applied to separate mobile sperm cells from stationary ones in a microfluidic system⁴⁷. However, chemotaxis based screening has been more challenging and very limited reports are available. In a study by Tai and colleagues, parallel collection channels were built to collect breast cancer cells that migrated across different distances towards a source of epidermal growth factor⁴⁸. However, operation of such a device is challenging and requires a delicate balance of the fluidic streams. There is a great need to develop novel protocols to isolate target cells from heterogeneous tissue cultures or mixed cell populations to support further molecular, genetic or proteomic phenotype identification.

In this study we develop a positive-selection screen for *S. typhimurium* virulence factors that inhibit DC chemotaxis in a diffusion-based microfluidic device with the potential for high-throughput capacity^{7, 44}. We had demonstrated previously that wild type (WT) *Salmonella* modulates the migration of DCs in transwell assays and in infected mice³. Because the chamber and microcapillary design of this device allows multiple cell populations to be monitored and separated on the basis of chemotactic abilities, we developed a chemotaxis-based screen using a library of *Salmonella* mutants. Our screen led to the identification of 7 *Salmonella* virulence factors that are involved in modulating DC chemotaxis towards CCL19, 5 of which were previously not implicated in this process. To our knowledge this study is the first reported use of a microfluidic device to conduct a genetic screen for bacterial effectors that influence the chemotaxis of mammalian cells.

Materials and Methods

Bacterial strains and culture conditions.

S. typhimurium SL1344 was transformed with the constitutive GFP-expression plasmid pFPV25.1⁴⁹ and this strain was used as the parent strain for all other *S. typhimurium* strains presented in this work. All *S. typhimurium* strains were cultured in Luria broth (LB) with 100 µg/ml carbenicillin at 37°C with constant agitation. All *S. typhimurium* gene deletion mutants (Table 1) were generated using the Datsenko and Wanner method⁵⁰. Briefly, 70 nucleotide primers were generated (IDT, San Diego, CA) such that the first 50 bases were complementary to the 3' or 5' end of the targeted gene and the last 20 bases were complementary to the P1 or P2 sites of pKD4 (flanking the kanamycin resistance gene, *kan*). These primers were used to PCR amplify the *kan* locus of pKD4, and the amplified DNA was purified and transformed in to *S. typhimurium* LT2 expressing λ Red recombinase. Recombinants were selected on 40 µg/ml Kan LB agar plate, and the resulting gene deletion mutations were moved to the GFP-expressing *S. typhimurium* background by P22 bacteriophage transduction. Deletion of the desired gene was confirmed by PCR amplification (Table 2) and DNA sequencing of the targeted gene (Mclab, South San Francisco, CA). For complementation of the *AsifA* mutant, the SifA expression vector *psifA* was transformed into the deletion mutant and transformants were selected on LB agar supplemented with 25 µg/ml chloramphenicol.

Cell culture.

Dendritic cells (DCs) were derived from mouse bone marrow based on the method of Lutz et al.⁵¹. Bone marrow was harvested from the femurs and tibia of 129X1/SvJ mice (Jax Mice, Bar Harbor, Me) between the ages of 6 and 12 weeks. Bone marrow cells were resuspended in Dulbecco's modified Eagle medium (DMEM) containing 10% heat-inactivated fetal bovine serum (FBS, Gibco), 50 mM β-mercaptoethanol, 1 mM HEPES, and 20 ng/ml granulocyte-macrophage colony-stimulating factor (GM-CSF, Peprotech, Rocky Hill, NJ). Approximately 20 million bone marrow cells were then seeded into a petri dish and incubated in a humidified chamber at 37°C and 5% CO₂. Two days later, 5 ml of DC culture medium was added to each plate and left to incubate for another 2 days. Finally, cells in suspension and loosely adhered to the plate were harvested and used for *S. typhimurium* infections 24 h later.

S. typhimurium-infection of DCs.

For time-lapse video microscopy experiments, the indicated *S. typhimurium* strain was grown overnight at 37°C with agitation, and approximately 2.5 billion bacteria were harvested, washed once with phosphate buffered saline (PBS), and then added to DCs at a multiplicity of infection (MOI) of 25:1. DCs were incubated with the *S. typhimurium* bacteria at 37°C for 30 min, and then the medium was changed to DC medium containing 100 µg/ml gentamicin to kill extracellular bacteria. After 1.5 h incubation the infected DCs were harvested by scraping in cold PBS and resuspended at 10 million cells/ml in DC medium containing 10 µg/ml gentamicin. Three µl of this cell suspension was injected into the cell-viewing chamber of the microfluidic device using a P20 micropipette, and the sink and source channels of the device were immediately flushed with 20 µl of DC medium.

Microfluidic Device Fabrication.

The microfluidic devices were fabricated using standard soft lithography protocols as previously described⁴⁵. Briefly, a two-layer SU8 (MicroChem Corp., Newton, MA) master consisting of a 10- μ m height capillary layer and a 100- μ m height chamber layer was fabricated on a silicon wafer (Fig. 1A), then treated with (3-aminopropyl) trimethoxysilane (Sigma, St. Louis, MO) as a release layer. To make polydimethylsiloxane (PDMS) devices, a 10:1 w/w mixture of Sylgard 184 monomer and hardener (Dow Corning, Corning, NY) was degassed under vacuum over the SU8 master and baked at 65°C for 1 h to cure. Inlet and outlet fluidic ports were punched out manually. Permanent bonding between PDMS chips and the cover glass was achieved by a 40-sec oxygen plasma treatment at 80 watts (Branson IPC oxygen plasma Asher, Hayward, CA).

Preparation of the microfluidic device.

On the day the microfluidic device was to be injected with DCs, the microfluidic device was first wetted using 70% ethanol and then washed with deionized sterile water. Next, the inside of the device was coated with 1 μ g/ml of mouse fibronectin for 3 h at room temperature. Just before injection of cells, the device was washed with DC medium containing 10 μ g/ml gentamicin.

Time-lapse video microscopy.

Twenty hours after injection into the microfluidic device, the infected DCs were subjected to a gradient of CCL19 or CXCL12 (Peprotech, Rocky Hill, NJ) by applying 200 ng/ml of the chemokine and 25 μ g/ml of 10 kDa dextran Texas Red (Invitrogen, Grand Island, NY) to the source channel at 3 μ l/h for the duration of the time-lapse video microscopy using a syringe pump (WPI, Sarasota, FL) and 100 μ l Hamilton gas-tight syringes (Hamilton, Reno, NV). Under similar conditions, Shamloo et al. measured the chemoattractant gradient concentration in the cell-viewing chamber to be linear, with maximum and minimum concentrations equal to 62% and 37%, respectively, of the source channel concentration⁴⁴. DC medium alone was supplied to the sink channel at an identical flow rate. The syringes were connected to the microfluidic device by PEEK tubing (IDEX Health & Science, Oak Harbor, WA). The DCs were imaged by DIC and fluorescence microscopy at 40X magnification on a Nikon Eclipse TE2000-E microscope with EMCCD camera. The device was placed on an automated stage and phase contrast and fluorescence images were taken and stored every 7 min for 5 h using Openlab software (PerkinElmer, Waltham, MA). Images were compiled into short videos using Volocity (PerkinElmer, Waltham, MA) and Quicktime (Apple, Cupertino, CA) softwares. The phase contrast videos were analyzed using ImageJ software (open source) with the plugins “Manual Tracking” and “Chemotaxis Tool” (Ibidi, Martinsreid, Germany). The Chemotaxis Tool was used to generate a chemotactic index and an average cell speed for every cell track and to make angular histogram plots for the cell track endpoints. Red fluorescence images taken of the 10 kD dextran Texas Red indicated that the chemical gradient was linear and stable throughout the 5 h duration of the time-lapse video microscopy.

Microfluidic-based screen.

A library of SPI2 effector gene deletion mutants was generated in the GFP-expressing *S. typhimurium* SL1344 (pFPV25.1) background using the method of Datsenko and Wanner described above⁵⁰. Each mutant was grown overnight at 37°C with agitation, and equal amounts of bacteria from each culture was combined into one tube and used to infect DC at a total MOI of 10:1. These DCs were resuspended at 100 million cells/ml and then injected into the device, the sink and source channels were flushed (in that order) to clear of cells, and the DCs were allowed to recover for 20 h in the incubator (as above). Next, the DCs were subjected to a gradient of CCL19 (as above) for 24 h. The source channel then was flushed with 200 μ l of 1% Triton X-100 in plain DMEM to retrieve DCs that had migrated through the capillaries and that remained associated with any part of the source channel. Five min incubation of these DCs in 1% Triton X-100 DMEM with agitation resulted in DC lysis, and the freed intracellular bacteria were spread onto LB agar plates containing 200 μ g/ml streptomycin, 40 μ g/ml kanamycin, and 100 μ g/ml carbenicillin. Colonies that grew overnight were cultured and used for genomic DNA isolation (Qiagen, Valencia, CA). The identities of the clones were determined by PCR and confirmed by DNA sequencing (as above). This screen was carried out 4 times and mutants that were isolated at least 3 out of the 4 screens were identified as positive mutants.

Statistics.

The threshold for positive selection in the screen presented here was isolation of the mutant in 3 out of 4 screens. For both cell speed and chemotactic index data, infected cells were compared to their uninfected neighbors within the same microfluidic device using the non-parametric rank-based Mann-Whitney test. The distribution of chemotactic indices and cell speed were tested for normality using the D’Agostino-Pearson test. The sample size (N) for the number of cells tracked for each treatment group was based on our initial experiments measuring chemotactic indices of uninfected DCs toward CCL19 (Fig. 1C). This sample group passed the test for normality and has a mean chemotactic index of 0.1742 (standard deviation = 0.3942) that is significantly different from 0 in both the non-parametric rank-based Wilcoxon signed-rank test ($p < 0.0001$) and a one-sample two-tailed Student’s t test ($p < 0.0001$). Initially we presumed that 0.1742 represented the true mean chemotactic index of this cell population (and 0.3942 was the true variance) and calculated the minimum N necessary for a given power ($1 - \beta$) and a type I error rate (α) of 0.05. For a power level of at least 0.8, N should be at least 43, and therefore more than 43 cells were tracked in every treatment group.

Table 1

SPI2 mutant	Primers used for gene deletion (5'-3')
<i>ΔssaV</i>	^{52*}
<i>ΔgogB</i>	ctaggttctaaatcttgctgaatgaaaataatgtaataatgatagctgtgtaggctggagctgcttc caataggctgctctatataataatataatgcatatttttaagcatatgaatatcctccttag
<i>ΔpipB</i>	ttgactcacacctataaggagctggctcacttcataagaaggaatcaaa gtgtaggctggagctgcttc agggggcctctgtttgaatactctgtttataaaatccctttatctcgacat gaatatcctccttag
<i>ΔpipB2</i>	atatgataaattttatcatgctgctgtgtctctcgggagaaaatgtgt aggctggagctgcttc cagattgtattcttacattgctttttatcagatttacgtcaaaaggcagat gaatatcctccttag
<i>ΔsopD2</i>	aatgagagcaacggattggatctgcttcgcggtaataatacaggagg gtgtaggctggagctgcttc aaaagcgtacaaaaggctccatcatcagtgggccttttaagactttc atatgaatatcctccttag
<i>ΔspvB</i>	caccgtaaaggaaacgctcatgcatattgatgtccgactgtaatgg ttaggctggagctgcttc gacctgactgaccgtaacaatgacattatcctcgagtaccgtaacagga catatgaatatcctccttag
<i>ΔspvC</i>	ggcggctcaggcgtgcccgttctctgcccctcctcccgaacagg cgtgtaggctggagctgcttc gtactccccggcgtggacggggtgtacctggccacattgtggatgag gcatatgaatatcctccttag
<i>ΔsteA</i>	cggctcagcagctgatttctaacaaaactggctaaacataaacgcttc atatgaatatcctccttag agaggagtaggacatataaagctattgagcaaatggaaggagtaggat gtgtaggctggagctgcttc
<i>ΔsteC</i>	ctgtagcgaatgtgccccggcattcgcagaaaagaacggaactaat gcatatgaatatcctccttag ttttatgtttgcatgtgtattataaaatctcagaggatgagacatgtga ggctggagctgcttc
<i>ΔsspH2</i>	^{52*}
<i>ΔsifA</i>	^{52*}
<i>ΔsifB</i>	^{52*}
<i>ΔspiC</i>	^{52*}
<i>ΔsseF</i>	^{52*}
<i>ΔsseG</i>	^{52*}
<i>ΔsseI</i>	3
<i>ΔsseJ</i>	^{52*}
<i>ΔsseK1</i>	ctaataatcatcatgtaaaatgtaatgaagtaagtaggacatttaattg ttgttaggctggagctgcttc cgaaactgatagttatgccaatattttatgtattcaatgacatgattatgcc atttccgcatatgaatatcctccttag
<i>ΔsseK2</i>	^{52*}
<i>ΔslrP</i>	^{52*}
<i>ΔsseL</i>	^{53*}

*The gene deletion mutation constructed in the referenced work was transduced into *S. typhimurium* SL1344 (pFPV25.1) for the experiments presented here.

Table 2

SPI2 mutant	Primers used for detection by PCR (5'-3')
<i>ΔssaV</i>	tagcaggattagctgaacgg aagccatcaataactcgccc
<i>ΔgogB</i>	cgctcagcatagctgctg gaagcagctccagcctacac
<i>ΔpipB</i>	tgaagcgtaaagctatgctgg gaagcagctccagcctacac
<i>ΔpipB2</i>	aaggcggcaacgagcgaat gaagcagctccagcctacac
<i>ΔsopD2</i>	gaatggttggcggctttg gaagcagctccagcctacac
<i>ΔspvB</i>	caggctttacgtgaggaacc gaagcagctccagcctacac
<i>ΔspvC</i>	cggtcagtcaggtcgtagcg gaagcagctccagcctacac
<i>ΔsteA</i>	tcagggttaatccctgcagg gaagcagctccagcctacac
<i>ΔsteC</i>	cgatgcgcttccaccagac gaagcagctccagcctacac
<i>ΔsspH2</i>	tccgggaatctttgtcgc atgtctgcccggacagatact
<i>ΔsifA</i>	gaacgtgacgtctgagaaa ccgcagttgagataaaaagg
<i>ΔsifB</i>	cgatgggcaacatgggataa gtttgtattgccagggga
<i>ΔspiC</i>	ggatgtggtgtgagcgaat ctggcataaagggtgaagtc
<i>ΔsseF</i>	agattccagaatgcgcaa tgaccattgggctaaccagg
<i>ΔsseG</i>	ggctgaaaatattgcgcct tgattccagcagcaaccgt
<i>ΔsseI</i>	gcgttgataccggatgatct tgttgtgtcgtatccacc
<i>ΔsseJ</i>	ggcattaacctcagctgttg gagctgtgtttgctcaagg
<i>ΔsseK1</i>	gctcactgtagggtattatg agcactcggattttaaagtgcc
<i>ΔsseK2</i>	ctcaggacttagcattgtgac gaagggtgagtaaaacaaggc
<i>ΔslrP</i>	ctctctcctcgctatgaaa agtattgacgagtagtgg
<i>ΔsseL</i>	acgtggcatgacagataac gtggttgaatcattgacggc

10

Results

Migration of infected DCs in a microfluidic device

Previous studies aimed at elucidating mechanisms of how pathogens influence immune cell migration have utilized transwells^{3, 54, 55}. For example, we previously demonstrated that *S. typhimurium* inhibits DC migration in transwells towards the chemokine CCL19³, and we identified a SPI2 effector, SseI that hinders DC migration³. We validated the use of the microfluidic device that maintains a stable gradient of CCL19 (Fig. 1A)⁴⁴ by comparing chemotaxis of uninfected DCs with *Salmonella*-infected DCs. Primary murine bone marrow-derived DCs were infected with WT *S. typhimurium* expressing green fluorescent protein (GFP) at a multiplicity of infection (MOI) of 25:1, conditions that lead to approximately 50% of the DCs being infected with *Salmonella*. The DCs were added to the fibronectin-coated cell culture chamber of the microfluidic device and allowed to recover for 20 h. After this time, the DCs were exposed to a stable CCL19 gradient by flowing DC medium with 200 ng/ml CCL19 through the source channel and DC medium alone through the sink channel at 3 μ l/h using a syringe pump⁴⁴. DIC and fluorescent images were taken every seven minutes for a total of five hours. DIC images were used to detect all DCs, and the fluorescent images were used to detect GFP-*Salmonella* and Dextran Texas Red, which was used as a tracer molecule to monitor the CCL19 gradient. We tracked DCs over a 5-h period and recorded each cell's speed, location, and overall angular direction of movement with respect to the CCL19 gradient. In the absence of a CCL19 gradient, uninfected mature DCs did not preferentially move in any one angular direction (Fig. 1B). The chemotactic index of each cell's track was calculated as the ratio of the distance traveled in the direction of increasing CCL19 divided by the overall length of the cell's track. We compared the chemotactic indices (Fig. 1C) and angular directions (Fig. 1D) of infected DCs to uninfected cells from the same device, thereby providing an internal control for each individual assay. While uninfected DCs had a clear chemotactic response to the CCL19 gradient, DCs infected with WT *S. typhimurium* did not chemotax toward CCL19 (Fig. 1C and 1D). Importantly, the degree of chemotaxis inhibition did not correlate with the number of intracellular bacteria per DC (data not shown). These results are in agreement with our previous work demonstrating that WT *S. typhimurium* modulates DC migration³. Taken together, our results validate the use of this microfluidic device to measure the chemotactic behavior of *Salmonella*-infected DCs. A representative video of DCs infected with WT *S. typhimurium* are available as supplementary material online (Supplementary Video). To test the robustness of the microfluidic device in these migration experiments, we also elucidated if *S. typhimurium* manipulates DC migration toward another chemokine, CXCL12. *Salmonella* also prevents the chemotaxis of infected DC toward CXCL12, confirming that this system can be used to study a range of host-pathogen interactions (Supplementary Fig. 1).

Since CCL19 is very important for migration to secondary lymphoid tissue for mature DCs^{6, 56, 57}, we focused on understanding what other *Salmonella* effectors modulate DC chemotaxis toward this chemokine. Our previous work identified

the *Salmonella* effector SseI, which is translocated into host cells by the SPI2 T3SS, as partially preventing DC migration. Therefore we reasoned that additional SPI2 translocated effectors may contribute to manipulating DC directed migration toward CCL19. To test this hypothesis, we infected DCs with an *S. typhimurium* strain that does not translocate any SPI2 effectors because it lacks a critical T3SS structural component (*Δ ssaV*)⁵⁸. In contrast to DCs infected with WT *Salmonella*, the DCs infected with this SPI2 T3SS-deficient mutant did chemotax toward CCL19 and were indistinguishable from uninfected DCs (Fig. 2A and 2B). The chemotactic indices of DCs infected with this SPI2 T3SS-deficient mutant were significantly higher than DCs infected with WT *Salmonella* ($p < 4.4 \times 10^{-3}$ in a Mann-Whitney test). These results demonstrate that the translocation of SPI2 effectors are responsible for the inhibition of DC chemotaxis toward CCL19. We next set out to identify these additional *Salmonella* effectors that are translocated into host cells by the SPI2 T3SS and influence DC chemotaxis towards CCL19.

Microfluidic-based genetic screen.

Individually testing each SPI2 effector mutant in a microfluidic migration assay would be laborious and time-consuming. Thus, we developed a positive-selection genetic screen, with the potential for high-throughput capacity, for *Salmonella* mutants that cannot block DC chemotaxis. We adapted the microfluidic device for this screen by enabling collection of cells that migrated through the microcapillaries into the source channel. We took advantage of the precise environment of the microfluidic device to screen a mutant library that consisted of a mixture of 20 different SPI2 effector gene deletion strains simultaneously (Fig. 3A). One of these strains contained a deletion of *spiC*, a gene that encodes a SPI2-encoded protein that is critical for the translocation of SPI2 effectors in vivo⁵⁹. Similar to *Δ ssaV*, SPI2 effector translocation into DCs is eliminated, enabling *Δ spiC* to function as a positive control for the screen. To conduct the screen, DCs were infected with the SPI2 effector mutant library at a MOI of 10:1 such that it would be highly unlikely for a single DC to be infected with two different mutants. The infected DCs were injected into the microfluidic device and allowed to recover for 20 h before exposure to a CCL19 gradient for 24 h. DCs that migrate towards CCL19 should either be uninfected or be infected with a *S. typhimurium* mutant lacking a SPI2 effector involved in inhibiting DC chemotaxis. To test this idea, DCs that migrated toward CCL19 through the capillaries and into the source channel after 24 h were harvested and lysed to free any intracellular bacteria. The lysate was plated on selective agar plates, and each *Salmonella* clone was subjected to conventional PCR techniques followed by sequencing for identification of individual SPI2 effector mutants (Fig. 3A).

To be considered a positive hit in this screen, a DC must migrate with sufficient speed and sufficient directionality to reach the sink channel within 24 h. Therefore, if DCs infected with WT or *Δ ssaV* mutant *Salmonella* migrated at different speeds in a CCL19 gradient, our screen could be biased towards detecting DCs infected with *Salmonella* that migrate faster, unrelated to their chemotactic abilities. We determined that while DCs infected with either WT or *Δ ssaV* migrated at a slower speed than uninfected DCs, their migration speeds were not significantly

different from each other (Fig. 3B). While it is biologically intriguing that *Salmonella* inhibits DC chemotaxis by a different mechanism than it decreases DC migratory speed, it is also beneficial because it allowed us to specifically screen for *Salmonella* mutants unable to inhibit DC chemotaxis.

To be sure that these target DCs had enough time to migrate into the source channel, we calculated the average distance a population of DCs infected with WT or Δ *ssaV* mutant *Salmonella* could travel in the direction of the CCL19 source channel after 5 h and 24 h (Fig. 3C). *Salmonella*-infected DCs must migrate at least the length of the capillaries (250 μ m) connecting the cell-viewing chamber to the source channel in order for the *Salmonella* bacteria to be captured inside of the source channel. While the average distance traveled in 5 h by DCs infected with Δ *ssaV* mutant *Salmonella* was only 57.5 μ m, in 24 h the DCs are predicted to travel an average distance of 275.9 μ m, which is sufficient to traverse the capillaries. Therefore, we selected 24 h as the time period for our chemotaxis screen. The average distance travelled by WT *Salmonella*-infected DCs was not significantly different from zero, but the distribution of these distances varied widely (Fig. 3C) such that a small fraction (0.08) of this DC population would still be able to reach the CCL19 source channel by 24 h. Based on these data, we reasoned that a DC would have an 8% chance of migrating into the source channel when infected with a *Salmonella* mutant still capable of inhibiting DC chemotaxis (similar to WT *Salmonella*). The probability that a DC infected with this same *Salmonella* mutant would migrate repeatedly into the source channel in at least 3 out of 4 repetitions of the screen may be calculated as $(0.08)^4 + 4(1 - 0.08)(0.08)^3 = 0.00193$, yielding an acceptably low false-positive error rate. Therefore, SPI2 effectors involved in inhibiting DC chemotaxis were only considered “positively selected” if they were detected in at least 3 out of the 4 screens (Fig. 3D, shaded).

We conducted the microfluidic chemotaxis screen four times and identified 58 individual SPI2 effector mutant clones (Fig. 3D). As expected, the Δ *sseI* mutant bacterial strain was isolated in 3 of the 4 screens, thus, validating the technique (Fig. 3D). In addition to Δ *sseI*, the *S. typhimurium* mutants Δ *sseF*, Δ *sifA*, Δ *sspH2*, Δ *slrP*, Δ *pipB2* and Δ *spiC* also were positively selected in the screen (Fig. 3D). While SpiC may be translocated into the DC cytoplasm⁶⁰, SpiC is also required for the formation of the translocon apparatus itself⁶¹ and Δ *spiC* mutants do not translocate SPI2 effectors in vivo⁵⁹. Thus, the Δ *spiC* mutant is phenotypically similar to Δ *ssaV* and its positive selection validates the screen. To further confirm the results of our high-throughput screening method, we infected DC separately with different SPI2 effector deletion mutants that were identified in the screen. In a series of separate microfluidic chemotaxis assays using only a single mutant strain per experiment, we confirmed that the mutants Δ *sseF*, Δ *sifA*, Δ *sspH2* and Δ *pipB2* did not inhibit DC chemotaxis toward CCL19 (Fig. 4). Importantly, the *sifA*-deletion strain containing a wild type copy of *sifA* on a plasmid (Δ *sifA*(*psifA*)) interfered with DC chemotaxis similar to wild type bacteria, verifying that the positive selection of the Δ *sifA* mutant in our screen was due to the specific lack of SifA (Fig. 4). Similar to our previously published results³, DC infected with the *sseI*-deletion strain containing a wild type *sseI* gene on a plasmid did not chemotax towards CCL19 (data not shown). Consistent with

our previous results, DC infected with the SPI2 effector mutants had reduced cell speed (Supplementary Fig. 2). In addition, as a negative control, we confirmed that DCs infected with a SPI2 effector mutant, Δ *sseK1*, which was not selected in the screen, had a chemotactic index similar to DCs infected with WT *Salmonella* (Fig. 4). Interestingly, DCs infected with the Δ *sseF* mutant bacterial strain chemotax towards CCL19 slightly better than their uninfected neighbors (Fig. 4), indicating our screen is sensitive enough to identify DCs with a range of chemotaxis phenotypes. It is intriguing that most of the effectors that were identified in the screen have been shown to interact, either directly or indirectly, with elements of the host cytoskeleton, which is essential for mammalian cell migration^{3, 62-67}.

Discussion

Microfluidic devices are now widely used in cell migration assays, because they provide precise, long-term control over the cellular microenvironment while still allowing direct observation^{41, 68}. However, despite the advantages these devices provide, they have not been adopted as screening platforms to identify genes from either the host or the pathogen that influence host cell migration. Here we present a method for performing a positive selection genetic screen for *Salmonella* translocated effectors that inhibit DC chemotaxis.

While microfluidic devices are commonly used in mammalian cell migration studies^{44, 69, 70}, to our knowledge they have not been used to study how pathogens influence immune cell migration. Using microfluidic devices allowed us to more precisely determine how *S. typhimurium* inhibits DC migration. Utilizing transwells, we previously demonstrated that *Salmonella* can hinder DC migration³, however, transwell data can be difficult to interpret because the effects on migratory speed and chemotaxis (directional migration) cannot be differentiated. Because chemokine gradients across a transwell membrane are only present for a short amount of time, any cellular perturbation that decreases migration speed potentially could be misinterpreted as a decrease in chemotaxis. This may be a particularly important consideration for studies of host-pathogen interactions, as all *Salmonella* infected DCs were found to have significantly decreased migration rates (Fig. 4 and Supplementary Fig. 1).

Through microfluidic migration assays, we confirmed that *Salmonella* attenuates DC chemotaxis toward CCL19 (Fig. 1) and CXCL12 (Supplementary Fig. 1). Recently, CCL19 was shown to have a much greater chemotactic potency than CXCL12 toward DCs⁷¹, and we have shown that SPI2 translocated effectors are completely responsible for *Salmonella*-dependent inhibition of chemotaxis toward CCL19 (Fig. 2).

To determine which SPI2 effectors target DC chemotaxis, we developed a high-throughput positive-selection genetic screen in our microfluidic device. We exploited the geometric design of the microfluidic device to screen for those DCs that were capable of efficient chemotaxis (Fig. 3). The chemotaxing cells can migrate through the microcapillaries to the source channel where they can be collected for genetic analysis. Our screen successfully identified two previously known and five new SPI2 effectors that are necessary for inhibiting DC chemotaxis toward CCL19 (Fig. 4).

It is striking that we identified several effectors involved in modulating host cell chemotaxis, and that all the single mutants have strong phenotypes. Our results indicate that the manipulation of DC directed migration by *Salmonella* is quite complex. It will be important to determine if the effectors that block DC chemotaxis work individually or together in a complex. It is likely that these factors, either separately or together, disrupt the ability of DCs to either sense or respond to the chemokine gradient. DCs sense CCL19 using the chemokine receptor CCR7⁷². Since *Salmonella*-infection does not compromise CCR7 expression by DCs⁷², it is likely that these SPI2 effectors target host factors downstream of CCR7 that help the cell respond to the CCL19 gradient. Stimulation of CCR7 by CCL19 leads to chemotaxis toward CCL19 and an increase in migratory speed⁷³. Chemotaxis toward a CCR7 ligand is controlled through a signaling module made up of heterotrimeric G proteins of the G_i subfamily and the MAPK protein family, whereas speed is governed by the Rho/Pyk2/cofilin module⁷³. Chemotaxis requires both actin filaments and microtubules, as well as a wide array of cytoskeletal regulatory proteins, to extend the plasma membrane forward and ultimately migrate in the direction of a chemical gradient^{74, 75}. Because SPI2 effectors mainly target DC chemotaxis and not migration speed, it is likely that they interfere with either the G_i/MAPK signaling module and/or the host cytoskeleton.

SseF, SifA, SspH2, PipB2, and SseI can interact directly or indirectly with the cytoskeleton^{3, 62-67, 76}. Both SseI and SspH2 interact with filamin, a F-actin cross-linking protein⁶⁶. SseI also binds to the cytoskeletal regulator and scaffolding protein, IQGAP1^{3, 77}. SseF and PipB2 both interact with the microtubule-associated molecular motors, dynein and kinesin-1, respectively^{62, 64, 65}. SifA also interacts with kinesin-1 indirectly by binding SKIP and is required for maintenance of the *Salmonella* containing vacuole (SCV) in DCs^{63, 78}. Except for SseI, all of these factors are required for *Salmonella*-dependent inhibition of antigen presentation in DCs⁷⁹, an activity that also requires a functional cytoskeleton⁸⁰. Understanding the molecular mechanism for how these *Salmonella* effectors (either separately or together) inhibit chemotaxis and whether it involves interactions with components of the host cytoskeleton is the subject of further study.

The current understanding of the main role of SPI2 effectors is to maintain the integrity and correct positioning of the SCV inside of the host cell during infection, partially through acting on the host cell cytoskeleton^{62-65, 67}. Here, we expand the role of SPI2 beyond the SCV to include the regulation of DC chemotaxis, potentially having important consequences for the host's immune response. In order to clear a *Salmonella* infection, the host must mount an adaptive immune response against this bacterial pathogen⁸¹, and immune cell migration along CCL19 gradients is essential to establishing an adaptive immune response⁸². However, a fraction of hosts fail to completely clear systemic *Salmonella* infections and become persistently infected⁸³. The results of our screen revealed that *Salmonella* targets the ability of DCs to chemotax toward CCL19 using a specific set of SPI2 effectors, and these results provide a potential mechanism for how these bacteria avoid clearance.

In addition to *Salmonella*, many other bacterial pathogens are

able to evade the host's immune response, often through translocating bacterial effectors directly into host cells⁸⁴. The microfluidic positive-selection screening method presented here is a novel, useful technique to identify bacterial effectors from many different pathogens that impact directed host cell migration toward a given chemokine. Additionally, this method could be adapted for increased capacity of high-throughput screening techniques. For example, by using DNA sequencing methods instead of conventional PCR techniques to identify mutants, much larger mutant libraries could be screened quickly and efficiently. These methods will allow researchers to determine which bacterial effectors are responsible for modulating host cell migration, which likely helps the bacteria regulate the host immune response. These effectors of immune cell migration may serve as excellent targets for future pharmaceutical development.

Beyond use in investigating host-pathogen interactions affecting host cell migration, this microfluidic-based screen can be adapted for general studies of mammalian cell chemotaxis. For example, mammalian cells could be screened for genes influencing chemotaxis using a retroviral insertion library and subjecting them to a gradient in the microfluidic device. Using negative selection, mutants that are unable to migrate towards the gradient could be identified by sequencing of the insertion site. This would provide a high-throughput mammalian cell chemotaxis screen that takes advantage of the precise control over gradient shape and stability provided by microfluidic devices. This genetic screening method will allow researchers to genetically probe increasingly complex questions concerning host cell chemotaxis and how pathogens manipulate that chemotaxis.

Conclusions

We have developed and validated a microfluidic-based positive selection genetic screening method and we have used this new method to investigate how a pathogen such as *Salmonella* alters host cell migration. Our screen successfully identified *Salmonella* effectors that are necessary for inhibiting DC chemotaxis toward CCL19 (Fig. 4), thereby expanding our understanding of how this pathogen manipulates the host cell and potentially the immune response. However, we believe this new tool is not limited to the study of host-pathogen interactions, but instead is broadly applicable to the study of cell migration in potentially any biological system.

Acknowledgements

We thank Manuel Amieva for his help and expertise with live-cell time-lapse video microscopy, data analysis and very helpful discussions. We thank Amir Shamloo for his help with computational analysis of time-lapse video microscopy data. We also thank Nicole Romano for her preparation of the detailed schematic of the microfluidic device, as well as Andrea Almaguer for her assistance with DC infection and migration measurements. We thank Sam Miller for providing *psifA* for complementation studies. Denise Monack, Ph.D. holds an Investigator in the Pathogenesis of Infectious Disease Award from the Burroughs Wellcome Fund. Additional support was provided by NIH 1-T32-HL098049 to Stanford Cardiovascular Institute (H.X.), and NIH DP2-OD006477 (S.C.H.). Sarah Carden

is supported by the Lucille P. Markey Stanford Biomedical Research Graduate Fellowship. The funders had no role in study design, data collection and analysis, decision to publish, or preparation of the manuscript.

5

Author Contribution

Conceived and designed the experiments: LMM, HX, SCH, DMM. Performed the experiments: LMM, SEC, HX. Analyzed the data: LMM, SEC, HX, SF, MR, SCH, DMM. Contributed reagents/materials/analysis tools: LMM, SEC, HX, SCH, DMM. Wrote the paper: LMM, SEC, DMM, HX.

Figure Legends

Figure 1: *S. typhimurium* inhibits DC migration along a gradient of CCL19 established inside a microfluidic device. A) The microfluidic chemotaxis device includes a cell culture chamber connected by microcapillaries to chemokine source and sink channels, which enable formation of a linear, stable chemokine gradient. Primary DCs were cultured, infected with GFP-expressing *S. typhimurium* and then injected into the microfluidic chemotaxis device. B) The angular histogram of uninfected mature DC tracks under a uniform distribution of CCL19 is shown. Angular histograms indicate the proportion of cells traveling in each direction when comparing a cell's final position to its initial position and subdivided into 10° bins. C and D) DCs infected with GFP-expressing WT *S. typhimurium* were cultured in CCL19 gradients and imaged by fluorescence and DIC microscopy every 7 min over the course of 5 h. The cell migratory tracks of infected DCs and their uninfected neighbors were used to calculate their chemotactic indices (C) and angular histograms (D). N is the number of individual cells tracked. Line and error bars represent the mean and SEM, respectively, and all P-values were determined using rank-based Mann-Whitney test.

Figure 2: *Salmonella* pathogenicity island 2 (SPI2) is required to inhibit DC chemotaxis toward CCL19. DCs infected with GFP-expressing WT or Δ *ssaV* (SPI2 mutant) *S. typhimurium* were cultured in a gradient of CCL19 and imaged every 7 min over 5 h. The chemotactic indices (A) and angular histograms (B and C) are presented. Line and error bars represent the mean and SEM, respectively, and n.s. (not significant) indicates P-value > 0.05 in a Mann-Whitney test.

Figure 3: Positive selection microfluidic-based genetic screen for SPI2 effector mutants unable to inhibit DC migration toward CCL19. A) A diagram of the microfluidic-based screen is presented. DCs were infected with a library of SPI2 effector mutants and allowed to migrate in a CCL19 gradient for 24 hours. DCs that migrated into the source channel were collected and lysed, and the *S. typhimurium* mutants were isolated as colonies. Mutants were identified by PCR and sequencing. B) DCs infected with either GFP-expressing WT or Δ *ssaV* *S. typhimurium* were cultured in CCL19 gradients and imaged by fluorescence and DIC microscopy every 7 min over the course of 5 h. The cell migratory tracks of both infected DC and their uninfected neighbors were recorded and used to calculate their

migration speed. The line represents the median, and all P-values were determined using the Mann-Whitney test. C) Predicted average distances traveled in the direction of the source channel by each DC infected with either Δ *ssaV* mutant or WT *Salmonella* were calculated by taking the product of each DC's chemotactic index and speed and the given amount of time (5 h or 24 h). Line and error bars represent the mean and SEM, respectively. Dashed black line drawn at $y = 250 \mu\text{m}$ (length of capillaries). D) The screen was repeated a total of 4 times and the number of times a given mutant was positively selected is indicated as "number of screens" and the total number of times a given mutant was isolated from the source channel over all the screens is indicated as "total number of clones isolated". The threshold chosen for positive selection was identification in 3 out of the 4 screen repetitions. Positively selected genes are shown in grey. The number of mutants collected ranged between 6 and 24 per screen.

Figure 4: SPI2 mutants positively selected by the microfluidic screen do not inhibit DC chemotaxis toward CCL19. DC infected with the indicated *S. typhimurium* strain were cultured in a gradient of CCL19 and imaged every 7 min over 5 h, and the chemotactic indices are shown here. *AsseK1* was not positively selected by the screen and serves as a control. *AsifA+(psifA)* refers to the complemented *AsifA* mutant. N is the number of individual cells tracked. Line and error bars represent the mean and SEM, respectively, and P-values were determined using the Mann-Whitney test and are indicated above the graph.

Supplemental Figure 1: *S. typhimurium* inhibits DC migration toward CXCL12 independently of SseI. A-D) DCs infected with GFP-expressing WT or Δ *ssel* *S. typhimurium* were cultured in a gradient of CXCL12 and imaged every 7 min over 5 h. The chemotactic indices (A) and angular histograms (B and C) are presented. A) Line and error bars represent the mean and SEM, respectively, and all P-values were determined using the Mann-Whitney.

Supplemental Figure 2: DCs infected with SPI2 mutants positively selected by the microfluidic screen have lower migratory speed compared to uninfected DCs. DCs infected with the indicated *S. typhimurium* strains were cultured in a gradient of CCL19 and imaged every 7 min over 5 h. The cell migratory tracks of both infected DC and their uninfected neighbors were recorded and used to calculate their speeds. N is the number of individual cells tracked. Lines represent the median, and P-values were determined using the Mann-Whitney test and are indicated above the graph.

Supplemental Figure 3: DCs located inside of the capillaries during time-lapse experiments do not affect the chemical gradient. A) Time-lapse images were taken every 84 min of the capillaries leading to the source channel in a chemical gradient containing CCL19 and 10 kD dextran Texas Red; DIC, red fluorescence images and plot profiles of the red fluorescence are shown (yellow outline denotes plot profile range, taken using imageJ). B) The number of DCs per capillary averaged over 3 separate videos (error bars indicate SEM). C) The speed of DCs infected with *AsifA(psifA)* *Salmonella* inside the capillaries (N =

6) compared to infected DCs in the cell-viewing chamber (bar indicates median speed).

Notes

§ Co-first authors

⁵ ^a Holy Names University, 3500 Mountain Blvd., Oakland, CA, USA.

^b Stanford University, 299 Campus Dr., Stanford, CA, USA.

^c Stanford Cardiovascular Institute, 476 Lomita Mall, Stanford, CA, USA.

† Corresponding author: dmonack@stanford.edu

References

1. M. M. Wang, E. Tu, D. E. Raymond, J. M. Yang, H. Zhang, N. Hagen, B. Dees, E. M. Mercer, A. H. Forster, I. Kariv, P. J. Marchand and W. F. Butler, *Nat Biotechnol*, 2005, **23**, 83-87.
2. R. Figueira and D. W. Holden, *Microbiology*, 2012, **158**, 1147-1161.
3. L. M. McLaughlin, G. R. Govoni, C. Gerke, S. Gopinath, K. Peng, G. Laidlaw, Y. H. Chien, H. W. Jeong, Z. Li, M. D. Brown, D. B. Sacks and D. Monack, *PLoS Pathog*, 2009, **5**, e1000671.
4. M. J. Worley, G. S. Nieman, K. Geddes and F. Heffron, *Proc Natl Acad Sci U S A*, 2006, **103**, 17915-17920.
5. K. Schumann, T. Lammernann, M. Bruckner, D. F. Legler, J. Polleux, J. P. Spatz, G. Schuler, R. Forster, M. B. Lutz, L. Sorokin and M. Sixt, *Immunity*, 2010, **32**, 703-713.
6. M. H. Jang, N. Sougawa, T. Tanaka, T. Hirata, T. Hiroi, K. Tohya, Z. Guo, E. Umemoto, Y. Ebisuno, B. G. Yang, J. Y. Seoh, M. Lipp, H. Kiyono and M. Miyasaka, *J Immunol*, 2006, **176**, 803-810.
7. H. Xu and S. C. Heilshorn, *Small*, 2013, **9**, 585-595.
8. K. Chung, M. M. Crane and H. Lu, *Nature methods*, 2008, **5**, 637-643.
9. C. B. Rohde, F. Zeng, R. Gonzalez-Rubio, M. Angel and M. F. Yanik, *Proc Natl Acad Sci U S A*, 2007, **104**, 13891-13895.
10. S. Takayama, E. Ostuni, P. LeDuc, K. Naruse, D. E. Ingber and G. M. Whitesides, *Nature*, 2001, **411**, 1016.
11. R. W. Applegate, Jr., J. Squier, T. Vestad, J. Oakey, D. W. Marr, P. Bado, M. A. Dugan and A. A. Said, *Lab Chip*, 2006, **6**, 422-426.
12. M. P. MacDonald, G. C. Spalding and K. Dholakia, *Nature*, 2003, **426**, 421-424.
13. A. E. Saliba, L. Saias, E. Psychari, N. Minc, D. Simon, F. C. Bidard, C. Mathiot, J. Y. Pierga, V. Fraissier, J. Salamero, V. Saada, F. Farace, P. Vielh, L. Malaquin and J. L. Viovy, *Proc Natl Acad Sci U S A*, 2010, **107**, 14524-14529.
14. H. Sugino, K. Ozaki, Y. Shirasaki, T. Arakawa, S. Shoji and T. Funatsu, *Lab Chip*, 2009, **9**, 1254-1260.
15. C. Lee, J. Lee, H. H. Kim, S. Y. Teh, A. Lee, I. Y. Chung, J. Y. Park and K. K. Shung, *Lab Chip*, 2012, **12**, 2736-2742.
16. Y. C. Tan, J. S. Fisher, A. I. Lee, V. Cristini and A. P. Lee, *Lab Chip*, 2004, **4**, 292-298.
17. X. Wang, S. Chen, M. Kong, Z. Wang, K. D. Costa, R. A. Li and D. Sun, *Lab Chip*, 2011, **11**, 3656-3662.
18. H. Wei, B. H. Chueh, H. Wu, E. W. Hall, C. W. Li, R. Schirhagl, J. M. Lin and R. N. Zare, *Lab Chip*, 2011, **11**, 238-245.
19. B. Yao, G. A. Luo, X. Feng, W. Wang, L. X. Chen and Y. M. Wang, *Lab Chip*, 2004, **4**, 603-607.
20. M. Chabert and J. L. Viovy, *Proc Natl Acad Sci U S A*, 2008, **105**, 3191-3196.
21. X. Hu, P. H. Bessette, J. Qian, C. D. Meinhart, P. S. Daugherty and H. T. Soh, *Proc Natl Acad Sci U S A*, 2005, **102**, 15757-15761.
22. T. M. Keenan, Hsu, C. H., Folch, A., *Applied Physics Letters*, 2006, **89**.
23. N. Bhattarjee, N. Li, T. M. Keenan and A. Folch, *Integr Biol (Camb)*, 2010, **2**, 669-679.
24. B. G. Chung, F. Lin and N. L. Jeon, *Lab Chip*, 2006, **6**, 764-768.
25. W. Saadi, S. Rhee, F. Lin, B. Vahidi, B. Chung and N. Jeon, *Biomedical Microdevices*, 2007, **9**, 627-635.
26. M. T. Breckenridge, T. T. Egelhoff and H. Baskaran, *Biomed Microdevices*, 2010, **12**, 543-553.
27. D. Irimia, G. Charras, N. Agrawal, T. Mitchison and M. Toner, *Lab on a Chip*, 2007, **7**, 1783-1790.
28. J. L. Haddox, I. W. Knowles, C. I. Sommers and R. R. Pfister, *Journal of Immunological Methods*, 1994, **171**, 1-14.
29. X. Cao and M. S. Shoichet, *Neuroscience*, 2001, **103**, 831-840.
30. A. P. Wong, R. Perez-Castillejos, J. Christopher Love and G. M. Whitesides, *Biomaterials*, 2008, **29**, 1853-1861.
31. S.-Y. Cheng, S. Heilman, M. Wasserman, S. Archer, M. L. Shuler and M. Wu, *Lab on a Chip*, 2007, **7**, 763-769.
32. H. Wu, B. Huang and R. N. Zare, *Journal of the American Chemical Society*, 2006, **128**, 4194-4195.
33. V. V. Abhyankar, M. A. Lokuta, A. Huttenlocher and D. J. Beebe, *Lab on a Chip*, 2006, **6**, 389-393.
34. J. Diao, L. Young, S. Kim, E. A. Fogarty, S. M. Heilman, P. Zhou, M. L. Shuler, M. Wu and M. P. DeLisa, *Lab on a Chip*, 2006, **6**, 381-388.
35. J. Adler, *Science*, 1966, **153**, 708-716.
36. R. A. Colvin, T. K. Means, T. J. Diefenbach, L. F. Moita, R. P. Friday, S. Sever, G. S. Campanella, T. Abrazinski, L. A. Manice, C. Moita, N. W. Andrews, D. Wu, N. Hacoheh and A. D. Luster, *Nat Immunol*, 2010, **11**, 495-502.
37. Z. Wang, Y. Kumamoto, P. Wang, X. Gan, D. Lehmann, A. V. Smrcka, L. Cohn, A. Iwasaki, L. Li and D. Wu, *J Biol Chem*, 2009, **284**, 28599-28606.
38. S. Boyden, *J Exp Med*, 1962, **115**, 453-466.
39. S. H. Zigmond, *Methods Enzymol*, 1988, **162**, 65-72.
40. D. Zicha, G. Dunn and G. ones, *Methods Mol Biol.*, 1997, **75**, 449-457.
41. D. Irimia, *Annu Rev Biomed Eng*, 2010, **12**, 259-284.
42. S. Paliwal, P. A. Iglesias, K. Campbell, Z. Hilioti, A. Groisman and A. Levchenko, *Nature*, 2007, **446**, 46-51.
43. A. Shamloo, H. Xu and S. Heilshorn, *Tissue Eng Part A*, 2012, **18**, 320-330.
44. A. Shamloo, N. Ma, M. M. Poo, L. L. Sohn and S. C. Heilshorn, *Lab Chip*, 2008, **8**, 1292-1299.
45. R. Onuki-Nagasaki, A. Nagasaki, K. Hakamada, T. Q. Uyeda, S. Fujita, M. Miyake and J. Miyake, *Lab Chip*, 2008, **8**, 1502-1506.
46. H. Hattori, K. K. Subramanian, J. Sakai, Y. Jia, Y. Li, T. F. Porter, F. Loison, B. Sarraj, A. Kasorn, H. Jo, C. Blanchard, D. Zirkle, D. McDonald, S. Y. Pai, C. N. Serhan and H. R. Luo, *Proc Natl Acad Sci U S A*, 2010, **107**, 3546-3551.

47. B. S. Cho, T. G. Schuster, X. Zhu, D. Chang, G. D. Smith and S. Takayama, *Analytical Chemistry*, 2003, **75**, 1671-1675.
48. W. Tai, C. F. Yeh, C. C. Wu and C. H. Hsu, in *15th International Conference on Miniaturized Systems for Chemistry and Life Sciences* Seattle, Washington, USA, 2011.
49. R. H. Valdivia, A. E. Hromockyj, D. Monack, L. Ramakrishnan and S. Falkow, *Gene*, 1996, **173**, 47-52.
50. K. A. Datsenko and B. L. Wanner, *Proc Natl Acad Sci U S A*, 2000, **97**, 6640-6645.
51. M. B. Lutz, N. Kukutsch, A. L. Ogilvie, S. Rossner, F. Koch, N. Romani and G. Schuler, *J Immunol Methods*, 1999, **223**, 77-92.
52. T. D. Lawley, K. Chan, L. J. Thompson, C. C. Kim, G. R. Govoni and D. M. Monack, *PLoS Pathog*, 2006, **2**, e11.
53. A. Rytönen, J. Poh, J. Garmendia, C. Boyle, A. Thompson, M. Liu, P. Freemont, J. C. Hinton and D. W. Holden, *Proc Natl Acad Sci U S A*, 2007, **104**, 3502-3507.
54. C. Konradt, E. Frigimelica, K. Nothelfer, A. Puhar, W. Salgado-Pabon, V. di Bartolo, D. Scott-Algara, C. D. Rodrigues, P. J. Sansonetti and A. Phalipon, *Cell Host Microbe*, 2011, **9**, 263-272.
55. P. Rajashree, P. Supriya and S. D. Das, *Immunobiology*, 2008, **213**, 567-575.
56. J. Y. Humrich, J. H. Humrich, M. Averbeck, P. Thumann, C. Termeer, E. Kampgen, G. Schuler and L. Jenne, *Immunology*, 2006, **117**, 238-247.
57. K. Ouwehand, S. J. Santeagoets, D. P. Bruynzeel, R. J. Scheper, T. D. de Gruijl and S. Gibbs, *Eur J Immunol*, 2008, **38**, 3050-3059.
58. M. Hensel, J. E. Shea, B. Raupach, D. Monack, S. Falkow, C. Gleeson, T. Kubo and D. W. Holden, *Mol Microbiol*, 1997, **24**, 155-167.
59. J. A. Freeman, C. Rappl, V. Kuhle, M. Hensel and S. I. Miller, *J Bacteriol*, 2002, **184**, 4971-4980.
60. Y. Shotland, H. Kramer and E. A. Groisman, *Mol Microbiol*, 2003, **49**, 1565-1576.
61. X. J. Yu, K. McGourty, M. Liu, K. E. Unsworth and D. W. Holden, *Science*, 2010, **328**, 1040-1043.
62. G. L. Abrahams, P. Muller and M. Hensel, *Traffic*, 2006, **7**, 950-965.
63. L. Diacovich, A. Dumont, D. Lafitte, E. Soprano, A. A. Guilhon, C. Bignon, J. P. Gorvel, Y. Bourne and S. Meresse, *J Biol Chem*, 2009, **284**, 33151-33160.
64. T. Henry, C. Couillault, P. Rockenfeller, E. Boucrot, A. Dumont, N. Schroeder, A. Hermant, L. A. Knodler, P. Lecine, O. Steele-Mortimer, J. P. Borg, J. P. Gorvel and S. Meresse, *Proc Natl Acad Sci U S A*, 2006, **103**, 13497-13502.
65. V. Kuhle, D. Jackel and M. Hensel, *Traffic*, 2004, **5**, 356-370.
66. E. A. Miao, M. Brittnacher, A. Haraga, R. L. Jeng, M. D. Welch and S. I. Miller, *Mol Microbiol*, 2003, **48**, 401-415.
67. M. B. Ohlson, Z. Huang, N. M. Alto, M. P. Blanc, J. E. Dixon, J. Chai and S. I. Miller, *Cell Host Microbe*, 2008, **4**, 434-446.
68. S. Kim, H. J. Kim and N. L. Jeon, *Integr Biol (Camb)*, 2010, **2**, 584-603.
69. U. Haessler, M. Pisano, M. Wu and M. A. Swartz, *Proc Natl Acad Sci U S A*, 2011, **108**, 5614-5619.
70. J. Yan, V. Mihaylov, X. Xu, J. A. Brzostowski, H. Li, L. Liu, T. D. Veenstra, C. A. Parent and T. Jin, *Dev Cell*, 2012, **22**, 92-103.
71. B. G. Ricart, B. John, D. Lee, C. A. Hunter and D. A. Hammer, *J Immunol*, 2011, **186**, 53-61.
72. C. Cheminay, M. Schoen, M. Hensel, A. Wandersee-Steinhauser, U. Ritter, H. Korner, M. Rollinghoff and J. Hein, *Microb Pathog*, 2002, **32**, 207-218.
73. L. Riol-Blanco, N. Sanchez-Sanchez, A. Torres, A. Tejedor, S. Narumiya, A. L. Corbi, P. Sanchez-Mateos and J. L. Rodriguez-Fernandez, *J Immunol*, 2005, **174**, 4070-4080.
74. P. K. Mattila and P. Lappalainen, *Nat Rev Mol Cell Biol*, 2008, **9**, 446-454.
75. A. J. Ridley, *Cell*, 2011, **145**, 1012-1022.
76. C. R. Beuzon, S. Meresse, K. E. Unsworth, J. Ruiz-Albert, S. Garvis, S. R. Waterman, T. A. Ryder, E. Boucrot and D. W. Holden, *EMBO J*, 2000, **19**, 3235-3249.
77. H. Kim, C. D. White and D. B. Sacks, *FEBS Lett*, 2011.
78. L. Petrovska, R. J. Aspinall, L. Barber, S. Clare, C. P. Simmons, R. Stratford, S. A. Khan, N. R. Lemoine, G. Frankel, D. W. Holden and G. Dougan, *Cell Microbiol*, 2004, **6**, 1071-1084.
79. S. Halici, S. F. Zenk, J. Jantsch and M. Hensel, *Infect Immun*, 2008, **76**, 4924-4933.
80. K. K. Peachman, M. Rao, D. R. Palmer, M. Zidanic, W. Sun, C. R. Alving and S. W. Rothwell, *Immunol Lett*, 2004, **95**, 13-24.
81. J. Hess, C. Ladel, D. Miko and S. H. Kaufmann, *J Immunol*, 1996, **156**, 3321-3326.
82. E. Ziegler, F. Gueler, S. Rong, M. Mengel, O. Witzke, A. Kribben, H. Haller, U. Kunzendorf and S. Krautwald, *J Am Soc Nephrol*, 2006, **17**, 2521-2532.
83. D. M. Monack, D. M. Bouley and S. Falkow, *J Exp Med*, 2004, **199**, 231-241.
84. S. Bedoui, A. Kupz, O. L. Wijburg, A. K. Walduck, M. Rescigno and R. A. Strugnell, *J Immunol*, 2010, **184**, 2237-2242.

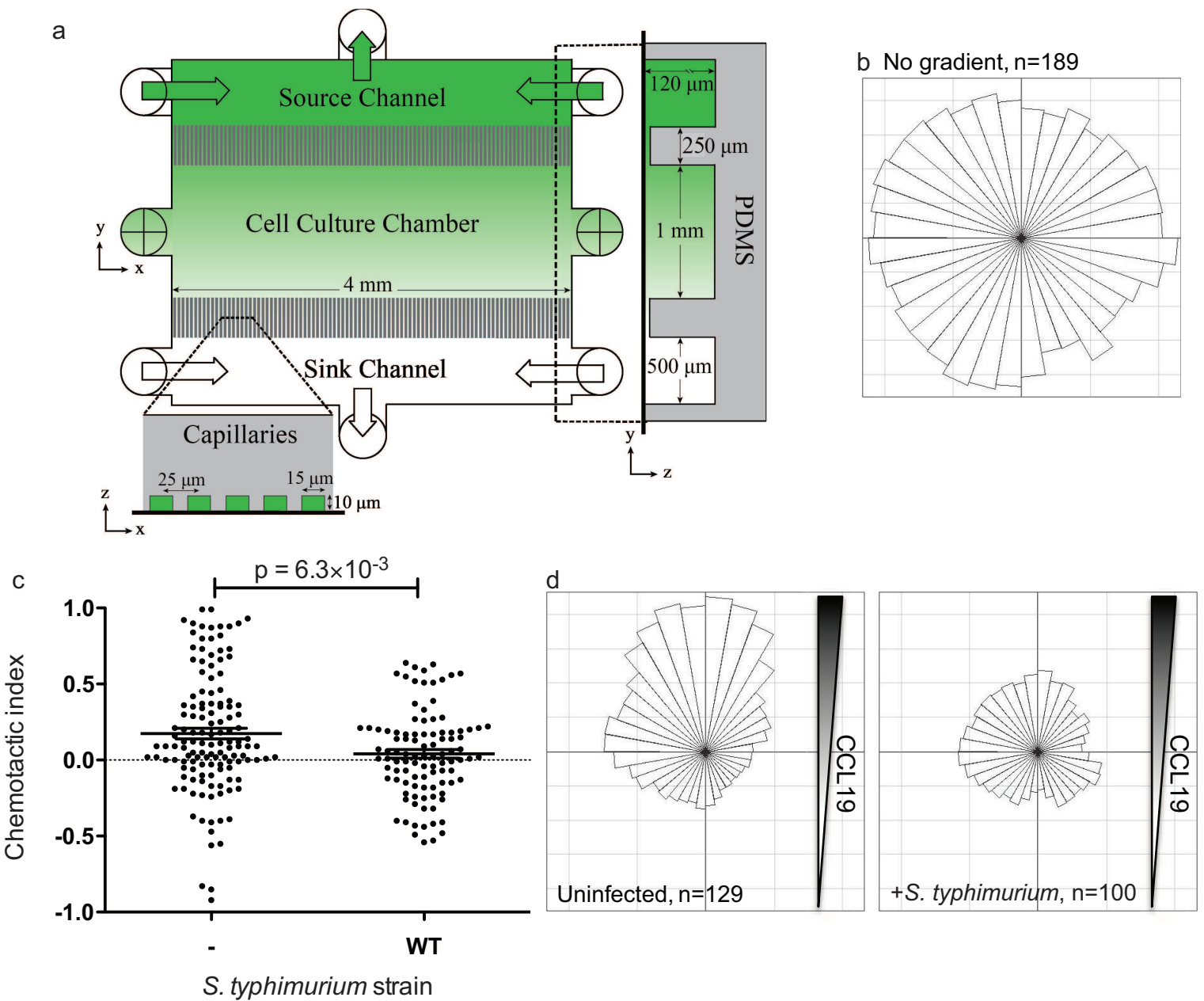


Figure 1

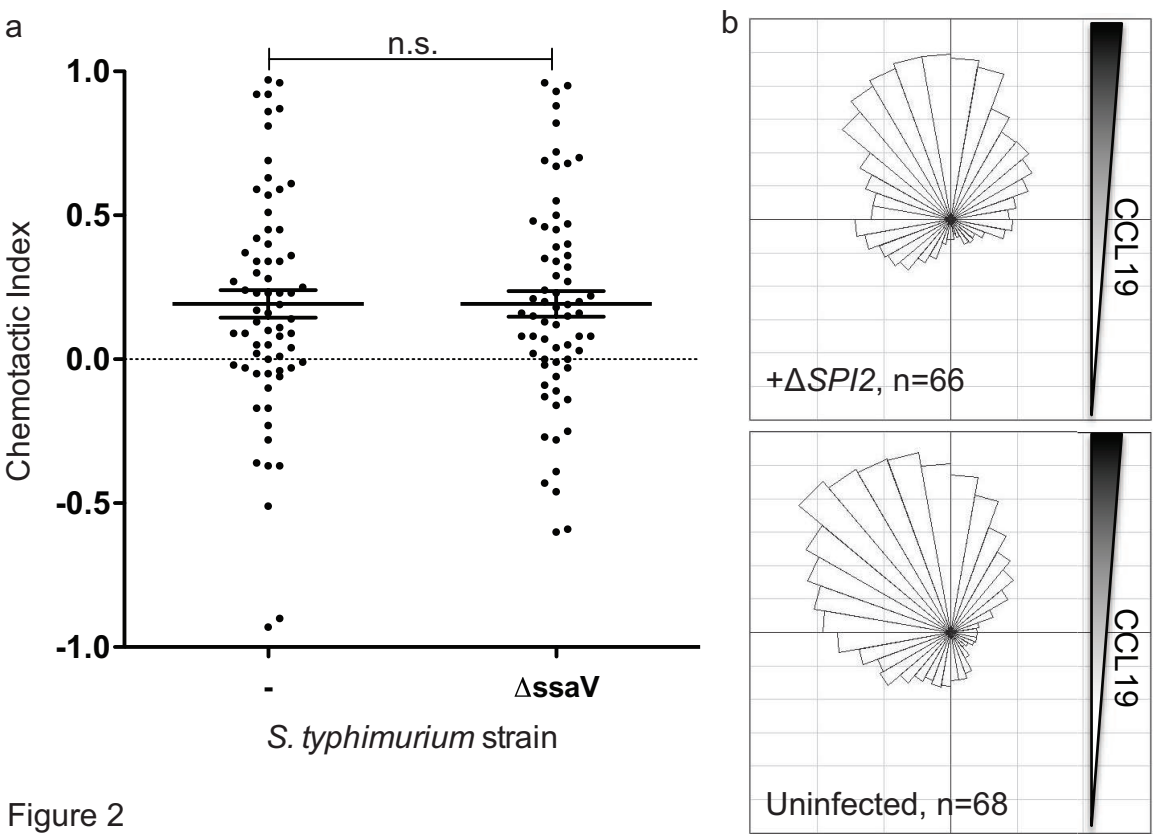


Figure 2

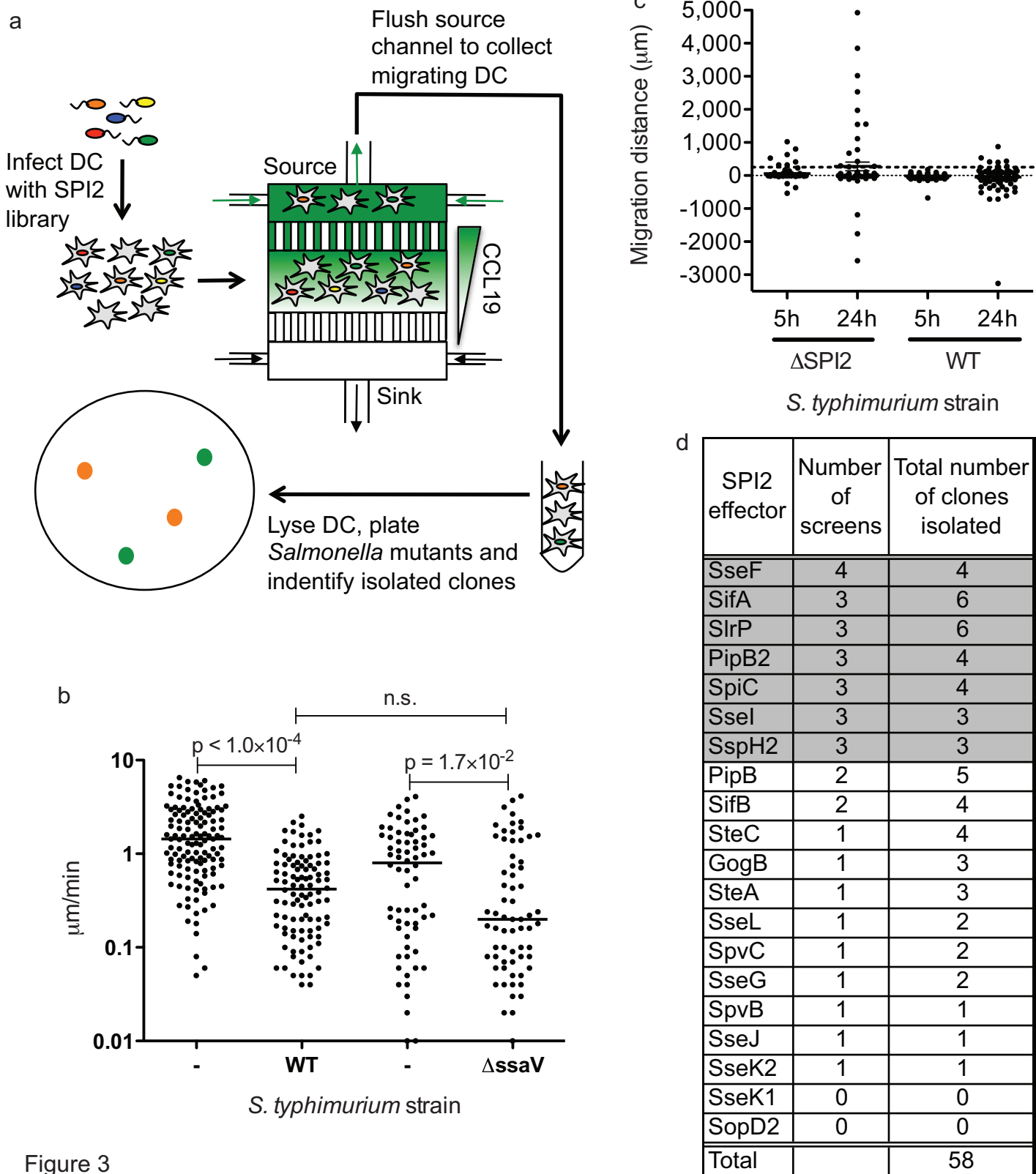


Figure 3

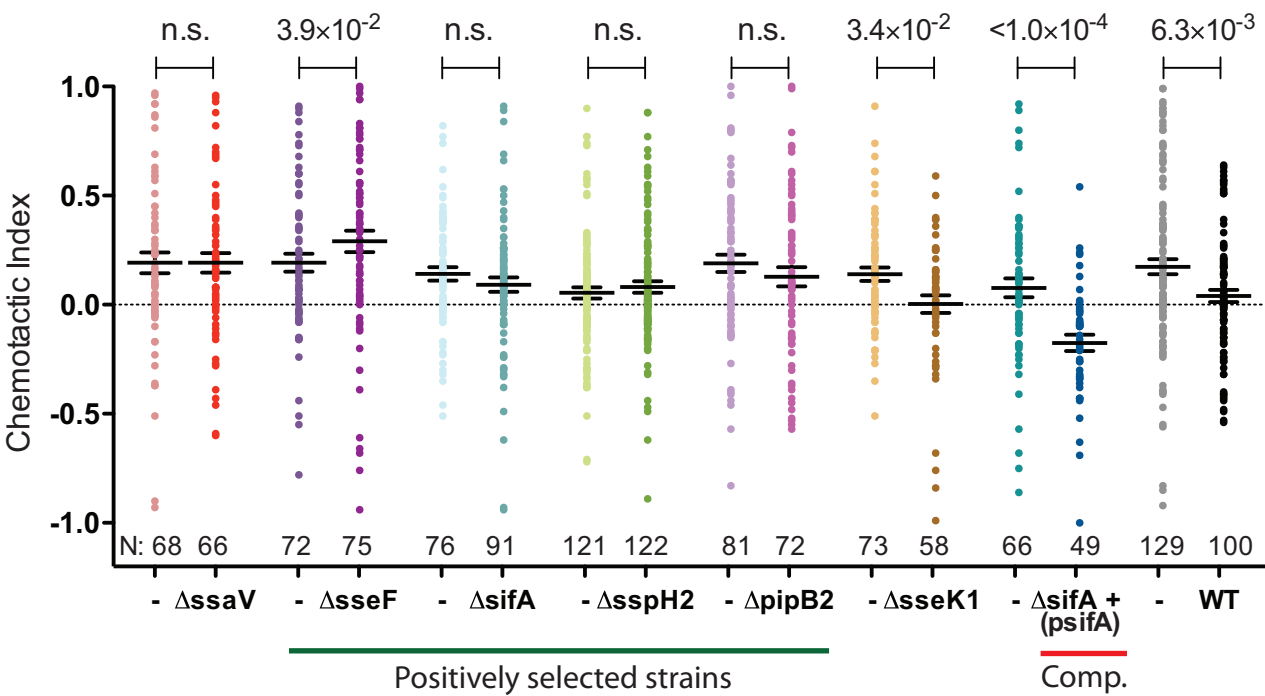
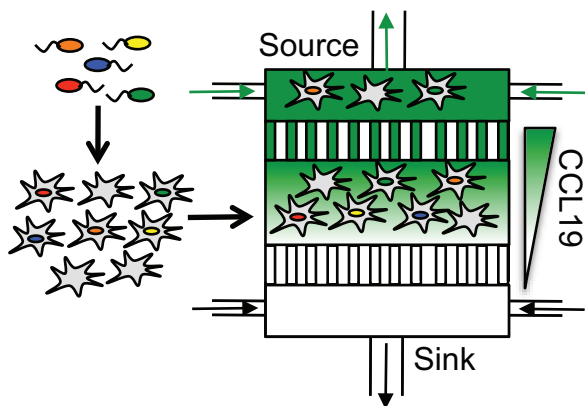


Figure 4



A microfluidic-based screen to identify *Salmonella* genes that impede dendritic cell chemotaxis, a critical step of the human immune response.